Kinetic Control of Nucleosome Displacement by ISWI/ACF Chromatin Remodelers

Ana-Maria Florescu,[1,2] Helmut Schiessel,[3] and Ralf Blossey[2]

[1]*Max-Planck Institute for the Physics of Complex Systems, Nöthnitzer Strasse 38, D-01187 Dresden, Germany*
[2]*Interdisciplinary Research Institute, Université des Sciences et des Technologies de Lille (USTL), CNRS USR 3078, 50, Avenue Halley, 59568 Villeneuve d'Ascq, France*
[3]*Instituut Lorentz voor de theoretische natuurkunde, Universiteit Leiden, P.O. Box 9506, NL-2300 RA Leiden, Netherlands*

(Received 20 March 2012; published 13 September 2012)

Chromatin structure is dynamically organized by chromatin remodelers, motor protein complexes which move and remove nucleosomes. The regulation of remodeler action has recently been proposed to underlie a kinetic proofreading scheme which combines the recognition of histone-tail states and the ATP-dependent loosening of DNA around nucleosomes. Members of the ISWI-family of remodelers additionally recognize linker length between nucleosomes. Here, we show that the additional proofreading step involving linker length alone is sufficient to promote the formation of regular arrays of nucleosomes. ATP-dependent remodeling by bidirectional motors is shown to reinforce positioning as compared to statistical positioning.

DOI: 10.1103/PhysRevLett.109.118103 PACS numbers: 87.14.gk, 87.15.A−, 87.16.Nn

Eukaryotic DNA is organized in the cell nucleus in the form of nucleosomes in which 147 base pairs (bp) of DNA are wrapped around a protein complex formed from, in general, eight histone proteins. Nucleosomes and the extranucleosomal (or linker) DNA form linear chromatin fibers that can undergo further packing into higher-order structures [1]. Apart from their role in chromatin condensation, the presence of nucleosomes directly affects transcription since they block the access to DNA. The molecular basis of nucleosome positioning is currently under intense scrutiny, combining efforts from structural biology, high-throughput genome and proteome experiments, single-molecule biophysics and modeling. Current attempts at an understanding of the underlying mechanism have uncovered three major levels: (i) sequence-dependence of nucleosomes via the associated elastic effects on DNA wrapping [2–4]; (ii) statistical positioning along DNA, for which nucleosomes are effectively considered as a one-dimensional fluid [5,6], and (iii), most recently, ATP-dependent chromatin remodeling [7–11]. Chromatin remodelers are multicomponent complexes performing multiple tasks on nucleosomes and DNA: recognition of histone tails and their modifications, recognizing linker DNA, and moving DNA around the nucleosomes. For this, they are equipped with an ATPase subunit (the motor), as well as specific recognition domains. For a review of remodeler properties, see [12]; a recent review of the currently known remodeler structures is [13]. In this Letter, we are concerned with the dimeric chromatin remodeler ACF, which is the abbreviation for ATP-utilizing chromatin assembly and remodeling factor, which belongs to the ISWI family of ATP-dependent chromatin-remodeling complexes [12]. These remodelers play an important role in gene repression by producing condensed chromatin. The remodeling capacity of ACF has recently been elucidated in a series of *in vitro* experiments by Narlikar *et al.* [14–16]. The model for ACF we propose exploits two essential ingredients observed in the experiments: (i) ACF is capable to override sequence-dependent positioning effects; (ii) the positioning of the nucleosome is performed by a linker-length dependent displacement mechanism, with the motor complex moving towards the longer linker length.

Kinetic proofreading of chromatin remodeling.—We begin by showing how the positioning mechanism of ACF fits into the recently postulated kinetic proofreading scheme of chromatin remodeling [17–19]. Active chromatin remodeling must be initiated by a recognition between remodeler and nucleosomal substrate. For the initial recognition of the nucleosomal substrate the chemical state of the histone tail, i.e., the presence or absence of enzymatic modifications, is crucial. The second step is the ATP-dependent action of the molecular motor which disrupts contacts between the wrapped DNA and the histone octamer. We write the remodeling reaction in the following scheme [19], where R represents the remodeler, N the nucleosome, I the remodeler-nucleosome complex, while I^* is the "activated" and I^T the translocated complex.

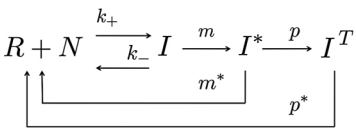

(1)

The reactions with rate m and p are irreversible since they involve ATP consumption. The reaction scheme is completed by the dissociation reactions from the activated intermediate state I^* and the translocated state I^T with rates m^* and p^*, respectively. It is straightforward to write down the rate equations for this reaction scheme [19]. Looking at the stationary states, one finds for the ratios of

products and educts the expression $[I^*]/([R][N]) = mk_+/[(k_- + m)(m^* + p)]$. Considering two reactions involving an incorrect (1) and a correct (2) substrate, following Hopfield [20] we can define the error fraction

$$F = \frac{[I_2^*]}{[I_1^*]} = \frac{m_2 k_{+,2}}{m_1 k_{+,1}} \frac{(k_{-,1} + m_1)}{(k_{-,2} + m_2)} \frac{(m_1^* + p_1)}{(m_2^* + p_2)}. \quad (1)$$

This scheme has recently been applied to a member of the ISWI family of remodelers, ACF [18,19]. ACF recognizes a basic patch on the N-terminal tail of histone H4. Based on recent experimental data [14–16,18], favored and disfavored reactions were shown to differ by a factor of $F \approx 300$ [19]. The capacity of ACF to recognize DNA linker-length is described in our model by a linker-length dependent translocation rate $p \equiv p(\ell)$, hence, it is useful to consider the ratio $[I^T]/[I^*] = p(\ell)/p^*$ and one can introduce an additional error fraction for left- or right-directed motion via

$$F_T = \frac{[I^T]_L}{[I^T]_R} = \frac{p(\ell)_L}{p(\ell)_R} \frac{p_R^*}{p_L^*} \frac{[I^*]_L}{[I^*]_R}. \quad (2)$$

According to the experiments by Narlikar *et al.,* neither the activation of the nucleosome nor the dissociation process depend on the translocation direction. One then has $(p_R^*/p_L^*)([I^*]_L/[I^*]_R) = 1$ and the error ratio becomes $F_T = p(\ell)_L/p(\ell)_R$, for the directional proofreading step.

In order to study remodeling of nucleosomes by ACF, we simulate nucleosome positioning by kinetic Monte Carlo simulations by considering activated nucleosome-remodeler complexes that move along a one-dimensional lattice in the presence of ATP. Simulation details are described in the Supplemental Material [21].

Single nucleosome positioning.—To calibrate our model we start with a single nucleosome to capture the nucleosome positioning experiments by Narlikar *et al.* which use a FRET analysis of nucleosomes on positioning sequences [14–16]; a similar modeling strategy for nucleosome remodeling has recently been employed by Forties *et al.* [22]. The displacement of the complex is, as is standard for motor complexes [23], assumed to occur with a Michaelis-Menten rate $p(\ell) = p_m(\ell)[\mathrm{ATP}]/([\mathrm{ATP}] + K_M)$, here with a K_M value of 11 μM. $p_{\mathbf{m}}$ is the maximum rate at saturation and is taken as dependent on linker-length ℓ according to

$$p_m(\ell) = \begin{cases} 0, & \text{if } \ell < \ell_{\min} \\ k_0 e^{a\ell}, & \text{if } \ell_{\min} < \ell < \ell_{\max} \\ k_0 e^{a\ell_{\max}}, & \text{if } \ell > \ell_{\max} \end{cases} \quad (3)$$

with the parameters $k_0 = 0.0059\ \mathrm{min}^{-1}$ (2 mM ATP), $a = 0.0911\ \mathrm{bp}^{-1}$ (2 mM ATP), $\ell_{\min} = 20$ bp, and $\ell_{\max} = 60$ bp. The values of $l_{\min}$ and $l_{\max}$ are taken from experiment; they refer to the DNA linker-sensitivity range of the ACF remodeler which is limited below due to steric reasons and limited above by remodeler size. Fitting the model to the data we need to determine the last free parameter which is the step size of the motor. We obtain the best agreement with a value of 13 bp, in accordance with [14], see Figure 1; a further data set is discussed in [21].

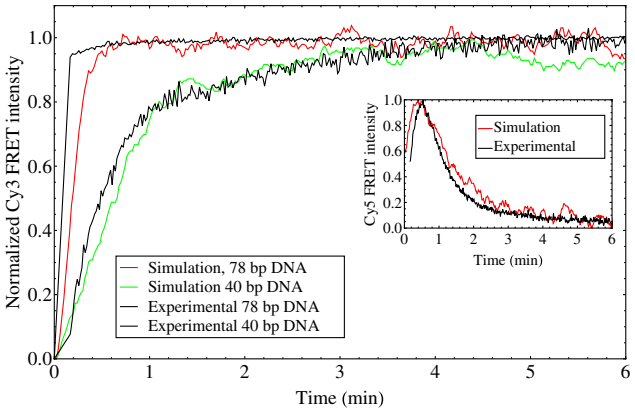

FIG. 1 (color online). Model fitting to normalized Cy3-FRET intensity I_N^F data from nucleosome positioning experiments on positioning sequences of different base composition and length, for an DNA-end positioned and a DNA-interior-positioned flurophore (inset). Forty and 78 bp refer to the length of the extranucleosomal DNA. See the Supplementary Material [14], and the Supplemental Material [21] to this Letter. The fit to experiment is performed by varying the still unspecified step size of the motor; the optimal result is obtained for a step size of 13 bp.

Nucleosome arrays.—We next use our calibrated model to study nucleosome arrays on a one-dimensional lattice of length L and show that the length dependence of p is crucial in generating a collective positioning effect. Based on our mononucleosome result yielding a step-size of 13 base pairs, we normalize our lattice by this length. A nucleosome thus occupies $S = 147\ \mathrm{bp}/13\ \mathrm{bp} = 11$ lattice sites. Fixed boundary conditions are imposed which are commonly used to model a strongly positioned nucleosome [5,6], as well as a minimal distance of two nucleosomes as given by one lattice site.

In order to limit the parameter space of all kinetic parameters in our proofreading scheme, we consider the set of three rates which we denote by $(k_{\mathrm{ads}}, k_{\mathrm{des}}, p)$. Here, the translocation rate p is either given as above, or we use a length-independent (constant) rate for comparison, with the value chosen as the maximal value of $p(\ell)$. The two rates k_{ads} and k_{des} collect all on- and off-rates of our proofreading scheme into effective adsorption and desorption rates, a notation inspired by [8]. In our case, we have $k_{\mathrm{des}} = m^* = p^*$, and $k_{\mathrm{abs}} = mk_+/(m + k_-)$ (see the Supplement for the derivation and the determination of parameter values). Further, we do not include explicit thermal sliding effects in our simulations, in contrast to, e.g., [8]. This is justified under the experimentally based assumption that the positioning of nucleosomes by ACF overrides DNA sequence dependence and hence sequence-dependent local free energy barriers are absent in our system. Only in the presence of such local barriers, thermal fluctuations can

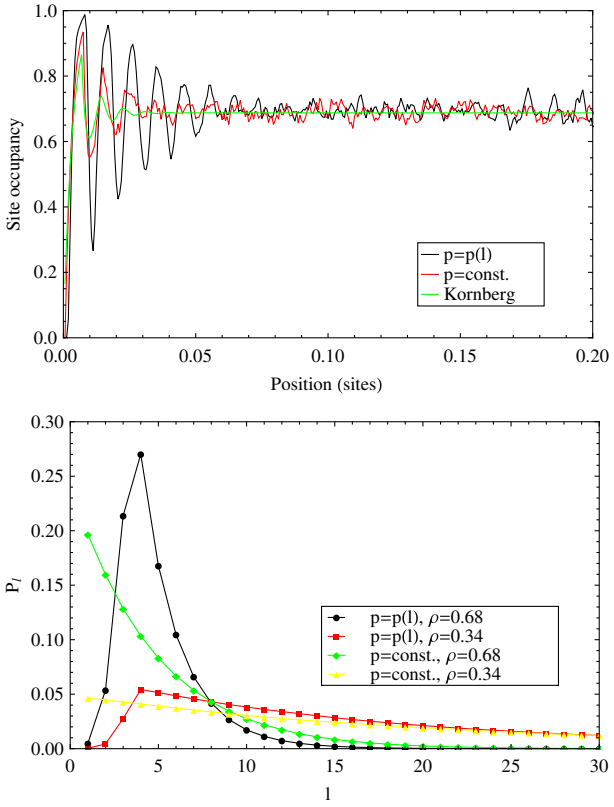

FIG. 2 (color online). Top: Site occupancy for a nucleosome array of 1600 sites with 100 nucleosomes, density $\varrho = 0.68$, after a simulation run of $t = 60$ min. Bottom: Distribution of linker lengths P_l at two densities and for both length-dependent and constant rates. All data were taken after individual runs for 60 min and sampling over 100 realizations.

distinguish between strong and weakly bound nucleosomes; without this sequence effect, they would simply result in an overall change in the translocation rate.

The rates k_{ads} and k_{des} allow us to distinguish two cases: an ideally processive remodeler, i.e., a motor that never falls off ($k_{\text{des}} = 0$) and a remodeler with variable processivity, modeled by a varying falloff rate. We begin with the ideal case. Figure 2 (top) shows the nucleosome occupancy of a DNA substrate (a "gene"), a one-dimensional lattice of sites $i = 1, ..., L$ with of $L = 1600$ lattice sites with $N = 100$ nucleosomes, i.e., at a fixed imposed density of $\varrho = 0.68$, with $k_{\text{des}} = k_{\text{abs}} = 0$. For comparison, we show the results of simulations with the constant maximal value of the rate, under otherwise identical conditions. With the length-dependent rate, remodeled nucleosomes appear more regularly positioned as with the constant rate. This is concluded from our finding that the positioning signal is not only more pronounced near the border, as the stronger peaks indicate, but it particularly spreads into the array over a longer distance. For further comparison, we also show the site occupancy curve obtained from the original statistical positioning model by Kornberg and Stryer [5]. The Kornberg-Stryer model for statistical positioning of nucleosomes was developed with the purpose of simulating nuclease digestion experiments. The nucleosomes are considered to be noninteracting, nonpenetrating and with fixed positions on DNA. The probability of a DNA site being free is computed by evaluating all possible configurations given by a fixed number of nucleosomes on a DNA sequence and weighing them. The resulting probability of nucleosome occupancy depends on the length of the DNA sequence, the number of sites each nucleosome occupies, and the mean total linker-length of DNA, which for our set up is $\langle l \rangle = (L - SN)/N = 5$ lattice units (65 bp). It is apparent that the statistical positioning signal is the weakest of the three considered.

To further quantify the effect due to the length-dependent rate, we have computed the distribution of linker lengths P_l over the array, where l is taken as the difference between the end positions of the nucleosomes. The result is shown in Figure 2 (bottom). The distribution peaks at $l = 4$ corresponding to a value of 52 bp. This value, which is close to the experimentally observed values [14], comes about by the fact that 4×13 bp is the largest integer <60 bp which we used for the sensitivity range of the remodeler: it is thus directly related to the properties of the remodeler itself, and may hence vary between different (remodeler) species. Data are shown, for comparison, for two densities and for both length and length-independent (maximal) rates. For smaller densities, the linker length distribution becomes more spread out but retains an exponential tail, while for a constant rate it is a pure exponential.

We now turn to the variably processive motor for which we allow the lattice to fill with given adsorption and desorption rates. Figure 3 (top) shows that for both constant maximal translocation rate and the length-dependent rate the obtainable maximal filling densities are essentially identical for both types of rates, except near $k_{\text{des}}/k_{\text{ads}} \approx 0$. For a constant translocation rate the maximal filling density for $k_{\text{des}} \to 0$ exceeds the value of the jamming density of a one-dimensional lattice, $\varrho_{\text{jamming}} \approx 0.75$ [24], and turns singular near $k_{\text{des}} = 0$. By contrast, even for $k_{\text{des}} = 0$, the length-dependent rate avoids jamming effects. With the knowledge of the attainable maximal densities for all rate ratios $k_{\text{des}}/k_{\text{ads}} \approx 0$, it suffices again to take density ϱ as our basic variable. This is demonstrated in Figure 3 (middle) which compares the two-point correlation function for a perfectly processive and a nonperfectly processive motor at about equal densities, with consistent results. The resulting difference in nucleosome positioning between the length-dependent and length-independent rates emerges clearly from the picture. A comparison to statistical positioning as obtainable from the Tonks gas leads to the same trend as found before from the Kornberg-Stryer result in the site occupancy [6]. While Fig. 3 (middle) refers to stationary profiles, we can also ask how the remodeler-nucleosome complexes behave in the initial transient before reaching stationarity. Considering the

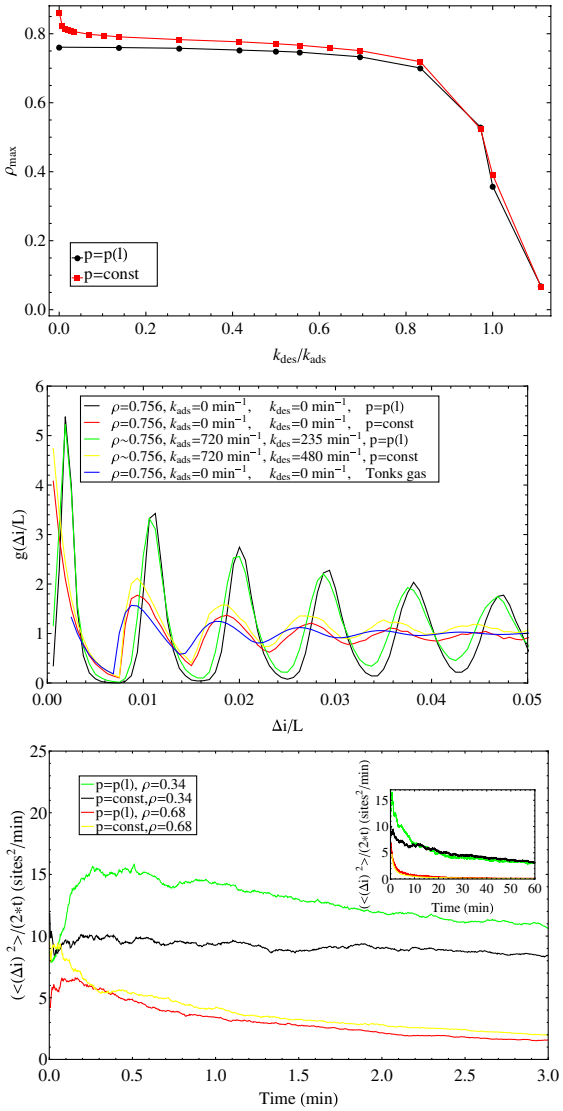

FIG. 3 (color online). Top: Maximal filling density of the array as a function of desorption (adsorption) rate ratio k_{des}/k_{ads}, for the two different translation-law models. Middle: Two-point correlation function for different rates, both for approximately similar densities in the presence of nucleosome adsorption (desorption), observed after 60 min of simulation. A comparison to the Tonks gas is also shown. Bottom: Effective diffusion coefficient of the first nucleosome in the array. Short-time and long-time behavior (see inset) for both translocation laws and for low and high filling densities.

motion of the first complex next to the boundary, we can determine the effective diffusion coefficient $D = \langle(\Delta i)^2\rangle/2t$, where $\langle(\Delta i)^2\rangle$ is the mean-squared deviation of the complex position on the lattice. We find that the initial regimes are characterized by a significant maximum of D at early times in the case of $p(\ell)$; the behavior is more pronounced at low densities. For long times, both constant and length-dependent rates display identical decay over time ultimately as $1/t$, with a density-dependent crossover-region (see inset).

Conclusions.—We have studied chromatin remodeling of nucleosome arrays with birectional remodelers like ISWI/ACF, based on experimental data available for single nucleosomes. The selection of remodeling direction is performed under conditions of ATP-dependent kinetic proofreading which, aside from targeting the proper nucleosome to be remodeled, also selects the proper DNA substrate for remodeler action. We find that positioning favors a distinct linker-length scale whose value is directly related to the molecular sensitivity range of the remodeler, the selection of which *in vivo* may also be related to the formation of higher-order structures. ATP-dependent remodeling favors positioning over a longer length scale than purely statistical positioning. ATP-dependent remodeling by ISWI/ACF can not be understood as a mere increase of temperature, in the sense that ATP-dependent processes facilitating positioning by helping the nucleosomes overcome energetic barriers of the underlying DNA sequence. Remodeling has been interpreted in the sense that the ATP-dependent processes help to position in a long-range (global) manner, while nucleosomes positioning themselves locally [25]. Our results show that the feature of directionality coupled to the proofreading scheme shows the appearance of an intrinsic long-range scale for the linker length. We conclude that details of the remodeler sensitivity range are relevant for large-scale nucleosome repositioning. We expect that the issue of local vs. global positioning effects due to remodelers will enable further advances also on still more global questions like the structure of the chromatin fibre. This will require an inclusion of sequence effects, neglected here on the basis of *in vitro* experiments on positioning sequences [14]. Given that the remodeler-based effect we describe here alone is enough to enhance positioning in the vicinity of a strong boundary, it is also immediately clear that multiple strongly positioned or "pinned" nucleosomes because of sequence-preferences will contribute to the creation of long-range ordered one-dimensional arrays. In this sense, active remodeling and sequence-based positioning are effects that can be viewed as acting in the same direction. Our model has been developed to describe, to a first approximation, the repression of a homogeneous chromatin state by ISWI/ACF remodelers. We have checked the robustness of this result against random variations of the translocation rate by up to 10% of its value. Such random variation of the translocation rate can be understood as arising from a heterogeneous chromatin environment. Our model is not meant to apply to highly heterogeneous chromatin states, as they may arise in many instances of transcriptional activation due to the presence of several activators and coactivators on the DNA fiber.

We thank G. J. Narlikar for allowing us to use her experimental data on the single nucleosome positioning. G. J. Narlikar, P. Korber, F. Pugh, J.-M. Victor, and the late J. Widom are thanked for discussion. A. M. F. thanks the MPG for support by a postdoctoral grant through the MPG-CNRS GDRE "Systems Biology."

[1] H. Schiessel, J. Phys. Condens. Matter **15**, R699 (2003).
[2] E. Segal *et al.*, Nature (London) **442**, 772 (2006).
[3] V. Miele, C. Vaillant, Y. d'Aubenton-Carafa, C. Thermes and T. Grange, Nucleic Acids Res. **36**, 3746 (2008).
[4] G. Chevereau, L. Palmeira, C. Thermes, A. Arneodo, and C. Vaillant, Phys. Rev. Lett. **103**, 188103 (2009).
[5] R. D. Kornberg and L. Stryer, Nucleic Acids Res. **16**, 6677 (1988).
[6] W. Möbius and U. Gerland, PLoS Comput. Biol. **6**, e1000891 (2010).
[7] V. B. Teif and K. Rippe, Nucleic Acids Res. **37**, 5641 (2009).
[8] R. Padinhateeri and J. F. Marko, Proc. Natl. Acad. Sci. U.S.A. **108**, 7799 (2011).
[9] Z. Zhang, C. J. Wippo, M. Wal, E. Ward, P. Korber, and B. F. Pugh, Science **332**, 977 (2011).
[10] T. Gkikopoulos *et al.*, Science **333**, 1758 (2011).
[11] A. Arnéodo *et al.*, Phys. Rep. **498**, 45 (2011).
[12] C. R. Clapier and B. R. Cairns, Annu. Rev. Biochem. **78**, 273 (2009).
[13] A. E. Leschziner, Curr. Opin. Struct. Biol. **21**, 709 (2011).
[14] J. G. Yang, T. S. Madrid, S. Sevastopoulos, and G. J. Narlikar, Nat. Struct. Mol. Biol. **13**, 1078 (2006).
[15] L. R. Racki, J. G. Yang, N. Naber, P. D. Partensky, A. Acevedo, T. J. Purcell, R. Cooke, Y. Cheng, and G. J. Narlikar, Nature (London) **462**, 1016 (2009).
[16] T. R. Blosser, J. G. Yang, M. D. Stone, G. J. Narlikar, and X. Zhuang, Nature (London) **462**, 1022 (2009).
[17] R. Blossey and H. Schiessel, HFSP J. **2**, 167 (2008).
[18] G. J. Narlikar, Curr. Opin. Chem. Biol. **14**, 660 (2010).
[19] R. Blossey and H. Schiessel, Biophys. J. **101**, L30 (2011).
[20] J. J. Hopfield, Proc. Natl. Acad. Sci. U.S.A. **71**, 4135 (1974).
[21] See Supplemental Material at http://link.aps.org/supplemental/10.1103/PhysRevLett.109.118103 for details.
[22] R. A. Forties *et al.*, Nucleic Acids Res. **39**, 8306 (2011).
[23] M. E. Fisher and A. B. Kolomeisky, Physica (Amsterdam) **274A**, 241 (1999).
[24] J. W. Evans, Rev. Mod. Phys. **65**, 1281 (1993).
[25] P. D. Partensky and G. J. Narlikar, J. Mol. Biol. **391**, 12 (2009).